Performance optimization of a thermoelectric generator element with linear, spatial material profiles in a one-dimensional setup

Knud Zabrocki[a)] and Eckhard Müller
Institute of Materials Research, German Aerospace Center (DLR), D-51170 Köln, Germany

Wolfgang Seifert and Steffen Trimper
Institute of Physics, University Halle-Wittenberg, D-06099 Halle, Germany

(Received 15 December 2010; accepted 15 March 2011)

Graded and segmented thermoelectric elements are studied in order to improve the performance of thermogenerators that are exposed to a large temperature difference. The linear thermodynamics of irreversible processes is extended by assuming spatially dependent material parameters like the Seebeck coefficient, the electrical and thermal conductivities. For the particular case in which these transport coefficients exhibit a constant gradient, we present an analytical solution of the one-dimensional thermal energy balance in terms of Bessel functions. Given linear spatial material profiles, we discuss the optimization of performance parameters like the electrical power P_{el} and the efficiency η of a graded thermogenerator element of fixed length and fixed boundary temperatures. The results are compared with the constant properties model, i.e., physically and chemically homogeneous material, as a suitable reference for performance evaluation.

I. INTRODUCTION

Although the direct conversion of heat flow into electrical power based on the occurrence of thermovoltage from a temperature difference known as the Seebeck effect, and likewise the inverse Peltier effect, which is the transport of heat directly linked to a current flow, have been discussed for a long time, there has been great progress in understanding these phenomena from a more microscopic point of view.[1,2] More recently the thermoelectric (TE) spin transfer in textured magnets[3] and the TE effect of Dirac fermions in graphene has been studied numerically.[4] Despite the effort in microscopic modeling, the application of linear thermodynamics of irreversible processes within a continuum approach is still under debate, especially for graded and segmented TE elements. They are characterized by locally nonconstant transport coefficients like the Seebeck coefficient, the electrical and thermal conductivities (see, e.g., Refs. 5 and 6). One aim of this study is to improve the performance of thermogenerators (TEGs) that are exposed to a large temperature difference. In 1909 Altenkirch[7] had already calculated the efficiency of a thermopile concerning the material properties that are needed to build practical devices. He provided the first evidence[7,8] that good TE materials should have a large Seebeck coefficient S, a high electrical conductivity σ (low electrical resistivity) to minimize Joule heat, and a low thermal conductivity κ to retain heat at the junctions and maintain a large temperature gradient. Later these qualitative aspects were embodied in the material figure of merit $z = S^2\sigma/\kappa$.[9] Note that there are correlations between the material coefficients like the Wiedemann–Franz law (connecting the electronic part of thermal conductivity and electrical conductivity) or Mott's formula, which links the Seebeck coefficient and electrical conductivity.[10–12] For metals the development of efficient TEGs can be traced to the thorough studies of the PbS–ZnSb compounds that were aimed to develop better material properties.[13,14] Even the description of a solar TEG is related to Refs. 15–17. The breakthrough of the theoretical description was due to Onsager's formulation of the physical principles underlying irreversible phenomena. This approach offered the basis for the theoretical description of TE effects.[18,19] The usage of semiconductors as TE materials led to a revival of TEs in the late 1950s that was due to Ioffe[9] and Goldsmid.[20] Because there had been no significant advances in improving the device efficiency or materials' figure of merit after the mid-1960s, the interest in thermoelectricity declined under the weight of inflated hopes after a very active period of investigations. The basic research in TEs stagnated for 30 years after that, as breakthroughs in the field decelerated; meanwhile some materials and commercial uses were still developed. New ideas and materials in the mid-1990s brought back TEs from niches into the focus of research. The search for green technologies, e.g., converting waste heat generated by car engines into usable power, pushes scientists to pick up "old" effects with new classes of materials exhibiting higher TE figures of merit to create practical applications using the advantages of TE power

[a)]Address all correspondence to this author.
e-mail: knud.zabrocki@dlr.de
DOI: 10.1557/jmr.2011.91

 © Materials Research Society 2011

https://doi.org/10.1557/jmr.2011.91 Published online by Cambridge University Press

generation.[21,22] A nice overview of different applications is given by Riffat and Ma.[23] Especially, the advantages of TE devices made them capable for applications in wide areas such as military, aerospace, measurement devices, and industrial or commercial products. Thus, TE solid-state equipment has no mobile parts and therefore needs much less maintenance. Other benefits are due to long-term steady-state operation time and an ecological point of view as the absence of chlorofluorocarbons. Otherwise, the efficiency of TE devices is lower in comparison to conventional coolers and engines. Nevertheless, in the age of global warming all possible ways of saving "waste" energy are welcome, independent of whether its origin is an industrial one or comes from such units like private cars, even if one should not overestimate their amount by using TE effects.[24] The efficiency of today's TE devices has to be improved not only by optimizing the material's performance itself but also by taking advantage of any option provided by special material design or functional grading of the material. To develop such high-performance functionally graded materials (FGM), the role of nanotechnology has been increased drastically.[21,22,25] There are different ways to model TE modules, depending on the length scale one is interested in. Whereas on a macroscopic scale the nonequilibrium thermodynamics attributable to Onsager is applicable,[18,19] on a mesoscopic scale and a microscopic scale the Boltzmann equation or a nonequilibrium quantum approach are appropriate tools.[22,26] In this article we focus on a continuum approach at a macroscopic scale. The TE material properties are in general both temperature and spatially dependent quantities,[27–30] although especially in engineering the focus is preferentially set on the determination of the temperature dependence of the material properties. This material's dependence on both implies two kinds of homogeneity (or inhomogeneity). On the one hand, a physically inhomogeneity is possible, i.e., the material's properties are temperature dependent; on the other hand, there is a chemical inhomogeneity in which you find the material's properties position dependent in a sample.[27,28,31] If mainly this T dependence is considered, one can express the material properties as spatial profiles over the length of a TE leg equivalently, as there is a steady temperature profile $T(x)$ available for any performance parameter in the one-dimensional (1D) steady state. Exemplarily, for the Seebeck coefficient, the spatial profile is then given by $S(x) = S[T(x)]$. It is well accepted that the material properties, in particular those of semiconductors, strongly depend on the carrier concentration that can be influenced by appropriate doping agents or a variation of the chemical composition.[9,32,33] Monitoring the carrier concentration opens the possibility of attaining a spatially dependent material, even if the temperature dependency is neglected. In this paper the material properties are assumed to be explicitly temperature independent (i.e., physically homogeneous) but spatially dependent (i.e., chemically inhomogeneous) to point out the quantitative effects of spatially dependent properties on, in particular, the performance parameters of a TEG with the efficiency η or the electrical power P_{el}. By that it is felt that these assumptions will provide an accurate mathematical model of the physical system while getting analytical solutions, yielding a better physical insight into the effect on the performance parameters concerning spatially dependent TE materials. Linear spatial profiles are among the basic approaches to finding the profiles that deliver optimum performance. The linear properties model (LPM) presented, as well as the constant properties model (CPM), i.e., a totally (chemically and physically) homogeneous material first considered for performance investigations by Ioffe,[9] is limited in comparison with really measured temperature dependent material. However, it can provide hints for optimized stacking schemes. Investigations similar to the present ones have already been performed.[34,35] Although these authors were successful in getting an analytical solution for the evolving temperature profile, the performance could not be determined quantitatively there because of the lack of suitable computation tools. Therefore, we revisit the corresponding solutions in particular to gain information about the influence of the slope of the material parameters on the performance. Furthermore, we calculate the corresponding optimal values in the particular case of linear spatial profiles as an example of FGM. In the present paper, we are able to compute the temperature profile $T(x)$ analytically within a "model-free setup" directly from the 1D thermal energy balance. It is assumed that all material profiles are independent of each other and have a *linear* spatial profile that is freely variable. The optimum current density and the optimum slopes for the profiles can be determined from the maximum of the global performance parameter under consideration while varying the current and slope. For arbitrary continuous and monotonous gradient functions of the material profiles $S(x)$, $\sigma(x)$, and $\kappa(x)$, the calculation of the temperature profile has been done numerically up to now by either a 1D TE finite element method code or the algorithm of multi-segmented elements.[36–38] Our analytical solution offers another reference, in addition to CPM, to test numerical procedures like that. Moreover, our results could also be the basis of a new multisegment algorithm based on LPM instead of CPM. Likewise, it can be used as the starting point for finding more generally shaped optimum profiles of the material properties. In the context of optimizing the performance by using graded material, the work of Bian et al. should be mentioned.[39,40] In their calculations the power factor $f = S^2\sigma$ was assumed to be constant, together with a high and constant thermal conductivity for which the end result is small overall temperature differences along the TE element.

Within the framework of a 1D steady-state model, our analysis is based on a single p-type TE element with fixed

https://doi.org/10.1557/jmr.2011.91 Published online by Cambridge University Press

length L and cross-sectional area A_c as part of a TEG.[37,41,42] A sketch of our model is shown in Fig. 1. Obviously the model will not capture all details of real materials such as the contact resistance, the nonparallel current flow, any heat loss perpendicular to the flow direction, and any heat loss due to convection or radiation. In this context, the following investigations are intended primarily for an "ideal" TE system.[41] Note that in this 1D description the spatial gradient is of course in the axial direction of the TE element (the direction of the heat flow and electrical current). With that we have the configuration of a longitudinal TEG.[43]

II. 1D THERMAL ENERGY BALANCE

TE effects are caused by the coupling of heat and charge transport that can be described within the framework of the linear response theory. For a detailed consideration, see Refs. 18 and 19. In particular for applications to TEs, see Refs. 27, 28 and 44–46. This approach is also denoted as Onsager–de Groot–Callen theory.[18,19,44,47–50] The transport of heat and charge is described by the corresponding current densities $\mathbf{q}$ (heat flow, heat flux) and $\mathbf{j}$ (electrical current density), respectively, which provide under isotropic conditions the linear constitutive relations

$$\mathrm{j} = \sigma\,\mathbf{E} - \sigma S \nabla T \quad , \tag{1a}$$

$$\mathbf{q} = \mathbf{q}_\kappa + \mathbf{q}_\pi = -\kappa \nabla T + S T j \quad , \tag{1b}$$

where $\mathbf{E}$ is the electric field, $\mathbf{q}_\kappa$ is the Fourier heat flux, $\mathbf{q}_\pi$ is the Peltier heat flux, and T is the temperature. (Normally, Q denotes the heat in units of 1 J, whereas with $\dot{Q} = \partial Q/\partial t$ the heat transfer rate or heat flow in units of 1 W is meant.

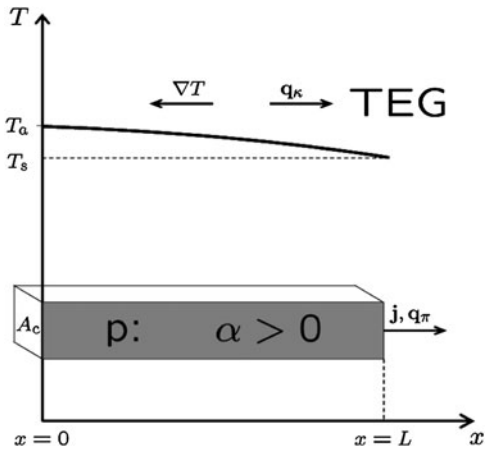


FIG. 1. One-dimensional setup of the TE element; notation of the vectors according to Eq. (1).

For the sake of simplicity the dot is sometimes ommitted. Often used is the heat flux, which is the heat transfer rate per cross-sectional area $q = 1/A_c\ \dot{Q} = (1/A_c)(\partial Q/\partial t)$ in units of 1 W/m^2.) Note that the Peltier heat flux has to be distinguished from what is phenomenologically known as the Peltier heat as occurring at a material transition; the latter represents just the divergence, i.e., the local rate of change of the first. The Peltier flux is treated here as a flux of thermal energy, although the energy transport does not actually take place as a transport of heat but of potential energy of the charge carriers. However, this energy can be made thermally apparent locally by introducing an (infinitesimally) thin layer with a vanishing Seebeck coefficient. The parameters S, σ, and κ are the aforementioned material parameters that generally depend on the temperature and the spatial coordinate. Under steady-state conditions the conservation of charge and energy leads to

$$\nabla \cdot \mathbf{j} = 0 \quad , \tag{2a}$$

$$\nabla \cdot \mathbf{q} = \mathbf{j} \cdot \mathbf{E} \quad . \tag{2b}$$

Assuming a 1D setup with constant electrical current density $\mathbf{j} = j\mathbf{e}_x$, Eq. (2a) is obviously fulfilled. From Eq. (1a) one easily deduces

$$E = \frac{j}{\sigma} + S\frac{\partial T}{\partial x} \quad , \tag{3}$$

with the first term representing the voltage drop because of the material's resistivity but the second representing an additional field due to the evolving thermovoltage. Inserting Eq. (1b) into Eq. (2b) and using Eq. (3), the local thermal energy balance reads as

$$\frac{\partial}{\partial x}\left(-\kappa\frac{\partial T}{\partial x} + STj\right) = \frac{j^2}{\sigma(x)} + jS\frac{\partial T(x)}{\partial x} \quad . \tag{4}$$

Similar calculations can be found in Refs. 28, 46, and 51–53. Equation (4) is just a 1D representation for isotropic material of Domenicali's 3D expression of the production of heat in an inhomogeneous, anisotropic medium, crystalline or otherwise (steady state).[27,28] The general material's dependence on the temperature T and the position $\mathbf{r}$, e.g., $S = S[\mathbf{r},T(\mathbf{r})]$, leads to a split-up of the derivative concerning the Peltier–Thomson term:

$$\nabla S[\mathbf{r}, T(\mathbf{r})] = \nabla S|_{T=\mathrm{const.}} + \left.\frac{\partial S}{\partial T}\right|_{\mathbf{r}=\mathrm{const.}}$$

$$\nabla T \Rightarrow \frac{dS}{dx} = \left.\frac{\partial S}{\partial x}\right|_{T=\mathrm{const.}} + \left.\frac{\partial S}{\partial T}\right|_{x=\mathrm{const.}}\frac{dT}{dx} \quad .$$

This split-up due to the chain rule corresponds to different physical heat fluxes: the (distributed) Peltier

https://doi.org/10.1557/jmr.2011.91 Published online by Cambridge University Press

heat $jT\,\partial S/\partial \mathrm{X}|_{T=\mathrm{const.}}$ and the Thomson heat $jT\,\partial S/\partial T|_{x=\mathrm{const.}} T'(x)$. Buist made the distinction between extrinsic and intrinsic Thomson heat for both terms.[54] In the 3D case there could be a third term if the electrical current density is spatial dependent, representing the so-called Bridgman heat. For the 1D case the steady-state condition $\nabla\cdot\mathbf{j} = 0$ leads to $\partial j(x)/\partial x = 0$, i.e., $j = \mathrm{const}$. The peculiarity of that equation is because the TE properties are playing a role twice here: first, thermal energy is absorbed or released according to the gradient of the Peltier coefficient ST (last term on the left side), but second, (right side) as a local energy conversion from or into electricity because of the current driven by or against the thermovoltage. Note that Eq. (4) can be understood in different ways because of the assumed type of the dependence of the material coefficients. If the parameters S, σ, or κ depend only on the temperature T but not explicitly on the spatial coordinate, i.e., we have a chemically homogeneous but physically inhomogeneous material, then Eq. (4) adopts the form

$$\kappa(T)T''(x) + \frac{d\kappa}{dT}T'^2(x) - j\tau(T)T'(x) = -\frac{j^2}{\sigma(T)} \quad , \quad (5)$$

which is a nonlinear differential equation for the unknown temperature profile $T(x)$. Here we have introduced the Thomson coefficient $\tau(T) = T\,dS/dT$. The differential equation has to be supplemented by boundary conditions. In 1D TE problems, Dirichlet boundary conditions can be applied, i.e., two fixed temperatures at the $x = 0$ and $x = L$ or mixed boundary conditions where a heat flux is given at $x = 0$. Throughout this paper, $T_\mathrm{a} = T(x = 0)$ is the temperature at the heat-absorbing side (hot side for TEG), whereas T_s denotes the heat sink temperature that is in many practical situations fixed close to room temperature. If the material parameters are supposed to be temperature dependent, averaged parameters can be defined by

$$\bar{S} = \frac{1}{T_\mathrm{s} - T_\mathrm{a}}\int_{T_\mathrm{a}}^{T_\mathrm{s}} S(T)dT \quad .$$

The temperature averages of further material parameters are defined in an analogous manner.

In the 1D steady state there is a one-to-one correspondence of the temperature T and the position x if the temperature profile is a continuous and strictly monotonous one. This especially applies for maximum efficiency and maximum power output of a TEG if constant or real, temperature dependent, material properties are considered. Then, there exists the inverse function $x(T)$ to $T(x)$. If these conditions are fulfilled, Eq. (5) can be transformed into

$$\kappa(x)T''(x) + \kappa'(x)T'(x) - jS'(x)T(x) = -\rho(x)j^2 \quad , \quad (6)$$

with $\rho(x) = 1/\sigma(x)$, where we presume spatial material profiles $S(x)$, $\sigma(x)$, and $\kappa(x)$ (see, e.g., Refs. 39, 46, 51, 52, and 55). Now the temperature dependence of the material parameters can be expressed by their spatial dependence leading to

$$\frac{1}{T_\mathrm{s} - T_\mathrm{a}}\int_{T_\mathrm{a}}^{T_\mathrm{s}} S(T)dT = \frac{1}{L}\int_0^L S(x)\frac{T'(x)}{(T_\mathrm{s} - T_\mathrm{a})/L}dx \quad , \quad (7)$$

with $S(x) = S[T(x)]$. As the function $LT'(x)/(T_\mathrm{s} - T_\mathrm{a})$ varies around unity, both the temperature average and the spatial average turn out to be close together for moderate gradients, where the spatial average will be defined as $S_\mathrm{av} = (1/L)\int_0^L S(x)dx$. As a consequence, we get for the Seebeck coefficient

$$\bar{S} \approx S_\mathrm{av} = \frac{1}{L}\int_0^L S(x)dx \quad ,$$

where the index "av" denotes the spatial average according to Eq. (7). Note that $\bar{S} = S_\mathrm{av}$ holds exactly for linear temperature profiles and in the CPM case, where the material properties are supposed to be constant and with it independent of the temperature and the position in the TE element. Naturally, Eq. (6) can also be used as an independent differential equation when the spatial dependence of the material parameters $S(x)$, $\sigma(x)$, and $\kappa(x)$ are the center of interest; see, for instance, Refs. 34, 35, and 38. Let us emphasize that, in contrast to Eq. (5), the differential equation Eq. (6) with spatially dependent material profiles is linear in T. This enables us to search for analytical solutions based on the principle of superposition.

In FGMs the whole set of material parameters may depend not only on the temperature but also on the local material quality that can be practically the composition of an alloy or the concentration of a dopant. For example, let us consider a single doped material or an alloy characterized by the concentration $c(x)$. Thus, the gradient of the Seebeck coefficient[53] S can be written as

$$\nabla S(T, c) = \frac{\partial S}{\partial c}\nabla c + \frac{\partial S}{\partial T}\nabla T \quad .$$

In 1D the gradient of the Seebeck coefficient reads $\nabla S = dS/dx\,\mathbf{e}_x$ if the single element profiles $c(x)$ and $T(x)$ are known, i.e.,

$$S(x) = S[c(x), T(x)] \quad .$$

Spatial material profiles may have a new quality: taking all local (implicit) dependencies into account, the graded TE material can be spatially dependent even under isothermal conditions. Note also that noncontinuously graded (i.e., segmented) elements are considered as FGM because they lead to the same functional effect.

https://doi.org/10.1557/jmr.2011.91 Published online by Cambridge University Press

III. ANALYTICAL SOLUTION FOR LINEAR SPATIAL PROFILES

Usually, a linear Seebeck profile (see Fig. 2) over the length of a TE element ($0 \le x \le L$) is given by

$$S(x) \equiv S(x; S_a, S_s, L) = S_a + \frac{\Delta S}{L} x \quad , \Delta S = S_s - S_a \quad , \quad (8)$$

where $S_a = S(x = 0)$ and $S_s = S(x = L)$ denote the Seebeck values at the boundaries. For our purpose we just take another description because we want to fix the (spatial) average of the Seebeck coefficient $S_{av} = L^{-1} \int_0^L S(x)dx = (S_a + S_s)/2$ to compare the results of the LPM with those of the CPM. Further, we define $\xi_S = S_a/S_s$ as the ratio of the boundary values of the Seebeck coefficient. Then, Eq. (8) can be transformed into

$$S(x) \equiv S(x; S_{av}, \xi_S, L) = \frac{2S_{av}}{1+\xi_S}\left[\xi_S + (1-\xi_S)\frac{x}{L}\right] = a(S)\xi_S + b(S)x \quad , \quad (9)$$

with

$$S_a = \xi_S \frac{2S_{av}}{1+\xi_S} \quad , \quad S_s = \frac{2S_{av}}{1+\xi_S} \quad .$$

Analogously, the thermal and electrical conductivities $\kappa(x)$ and $\sigma(x)$ can be defined containing the appropriate averages and ratios, κ_{av}, σ_{av}, $\xi_\kappa = \kappa_a/\kappa_s$ and $\xi_\sigma = \sigma_a/\sigma_s$, respectively. In addition, we use the abbreviations

$$a(y) = \frac{2y_{av}}{1+\xi_y} \quad \text{and} \quad b(y) = \frac{2y_{av}}{L}\frac{(1-\xi_y)}{(1+\xi_y)} = \frac{\Delta y}{L} \quad ,$$

where y stands for S, κ, or σ.

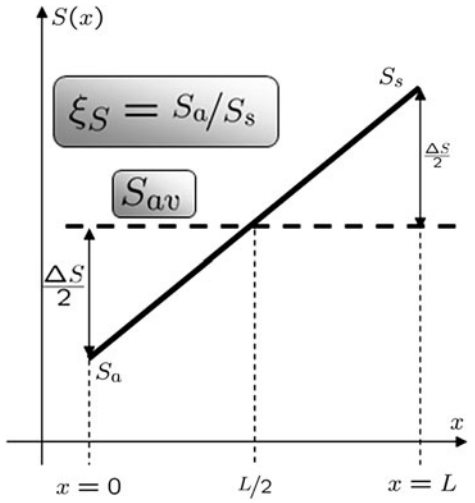


FIG. 2. Spatially linear profile of the Seebeck coefficient throughout the TE element; $S_{av} = L^{-1} \int_0^L S(x)dx = (T_a + T_s)/2$ and $\xi_S = S_a/S_s$.

The thermal energy balance Eq. (6) with the profiles defined according to Eq. (9) is an inhomogeneous differential equation having an analytical solution in the form of Bessel functions (see Appendix A). It is common knowledge that these functions have been found in a wide variety of physical problems. For an overview of this and the properties of these functions, see Refs. 56–60. The solution of the boundary value problem for the temperature profile for given ratios ξ_κ, ξ_S, and ξ_σ can be found as a sum of the general solution of the homogeneous equation and a particular solution of the inhomogeneous equation, see Appendix A and Tables I-III.

$$T(x) = C_1 Y_0\left(A\sqrt{\kappa(x)}\right) + C_2 J_0\left(A\sqrt{\kappa(x)}\right) + \frac{\pi j^2}{b(\kappa)}\left[J_0\left(A\sqrt{\kappa(x)}\right)\int_0^L \frac{Y_0\left(A\sqrt{\kappa(x)}\right)}{\sigma(x)}dx - Y_0\left(A\sqrt{\kappa(x)}\right)\int_0^L \frac{J_0\left(A\sqrt{\kappa(x)}\right)}{\sigma(x)}dx\right]$$

with

$$A \equiv -2\sqrt{\frac{-jb(S)}{b^2(\kappa)}} = -2L\sqrt{\frac{-j\Delta S/L}{(\Delta\kappa)^2}} \quad , \quad (10)$$

where Y_0 and J_0 are the Bessel functions, $\kappa(x)$, $\sigma(x)$ are taken as defined in Eq. (9). The free constants C_1 and C_2 can be fixed by boundary conditions. Particular solutions for different variants of given linear profiles are listed in Tables I-III.

IV. PERFORMANCE PARAMETERS OF A TEG AND CPM

Once having calculated $T(x)$, all performance parameters of interest can be determined as a function of the electrical current density j. In this paper we are concentrating on the electrical power P_{el} and on the efficiency η of a TEG, therewith continuing previous investigations on graded TEGs.[35,61–65]

In a 1D setup, the electrical power is given by[55]

$$P_{el} = \iiint \mathbf{j}\cdot\mathbf{E}\,dV = A_c\int_0^L \left[\rho j^2 + jS\frac{dT}{dx}\right]dx = A_c\int_0^L \pi(x)dx \quad ,$$

where $\pi = \mathbf{j}\cdot\mathbf{E}$ is the electrical power in a volume dV or the differential electrical power.[65] The power output of a TEG is defined here according to thermodynamic rules: quantities input to the system are positive. Hence, the net power output density (net electrical power output per cross-sectional area A_c) is

https://doi.org/10.1557/jmr.2011.91 Published online by Cambridge University Press

$$p_{\mathrm{net}}(j) = -p(j) = -P(j)/A_{\mathrm{c}} = -\int_0^L (\rho(x)j^2 + jS(x)T'(x))dx = -\int_0^L \pi(x)dx \quad . \tag{11}$$

Finally, the efficiency of a TEG is defined as the ratio between the electrical power output and the entering thermal power Q_{a},

$$\eta = \frac{-P_{\mathrm{el}}}{Q_{\mathrm{a}}} = \frac{p_{\mathrm{net}}}{q_{\mathrm{a}}} \quad \text{with} \quad q_{\mathrm{a}} = \frac{Q_{\mathrm{a}}}{A_{\mathrm{c}}} \quad , \tag{12}$$

where q_{a} is the absorbed thermal power density at $x = 0$ [see Eq. (1b) and Fig. 1].

Many of the previous works are related to the CPM (i.e., totally homogeneous material). For an approximation you can take the averaged values of the material properties, which means $S(x) = S_{\mathrm{av}}$, $\sigma(x) = \sigma_{\mathrm{av}}$, and $\kappa(x) = \kappa_{\mathrm{av}}$, and calculate the performance in the framework of CPM with these values. Note that there is another possibility of taking the constant coefficient for the thermal energy balance into account, e.g., by averaging the Thomson coefficient τ instead of the Seebeck coefficient, which is called the *method of averaged coefficient* (see Ref. 53, p. 276). In the following we will concentrate on the CPM and calculate the performance parameters from the resulting parabolic temperature profile

$$\frac{d^2T}{dx^2} = -\frac{j^2}{\kappa_{\mathrm{av}}\sigma_{\mathrm{av}}} \rightarrow T(x) = T_{\mathrm{a}} + \frac{T_{\mathrm{s}} - T_{\mathrm{a}}}{L}x + \frac{j^2}{2\kappa_{\mathrm{av}}\sigma_{\mathrm{av}}}x(L-x) \quad , \tag{13}$$

leading to the net power output density

$$p_{\mathrm{net}} = -\frac{P_{\mathrm{el}}}{A_{\mathrm{c}}} \rightarrow p_{\mathrm{net}}^{\mathrm{CPM}}(j) = jS_{\mathrm{av}}(T_{\mathrm{a}} - T_{\mathrm{s}}) - \frac{j^2L}{\sigma_{\mathrm{av}}} \quad , \tag{14}$$

which is nothing else than the difference between the TE voltage and the ohmic voltage drop. A straightforward calculation gives the efficiency η as a function of the electrical current density j (see Ref. 55):

$$\eta^{\mathrm{CPM}}(j) = \frac{jS_{\mathrm{av}}(T_{\mathrm{a}} - T_{\mathrm{s}}) - \frac{j^2L}{\sigma_{\mathrm{av}}}}{S_{\mathrm{av}}T_{\mathrm{a}}j - \kappa_{\mathrm{av}}\left(\frac{\partial T}{\partial x}\right)\big|_{x=0}} = \frac{2S_{\mathrm{av}}\sigma_{\mathrm{av}}(T_{\mathrm{a}} - T_{\mathrm{s}})Lj - 2L^2j^2}{2S_{\mathrm{av}}\sigma_{\mathrm{av}}T_{\mathrm{a}}Lj + 2\kappa_{\mathrm{av}}\sigma_{\mathrm{av}}(T_{\mathrm{a}} - T_{\mathrm{s}}) - L^2j^2} \quad . \tag{15}$$

An optimization of the performance parameters in the case of CPM due to j is a classical extreme value task. The external parameters like the geometry with L and A_{c} as well as the boundary temperatures T_{a} and T_{s} are kept fixed during this optimization. From the solution of the equations $\partial p_{\mathrm{net}}^{\mathrm{CPM}}/\partial j = 0$ and $\partial \eta^{\mathrm{CPM}}/\partial j = 0$ the optimum values for the current densities, where you find maxima for the performance parameters, are calculated as

$$j_{\mathrm{opt},p}^{\mathrm{CPM}} = \frac{S_{\mathrm{av}}\sigma_{\mathrm{av}}}{2}\frac{\Delta T}{L} \quad \text{and} \quad j_{\mathrm{opt},\eta}^{\mathrm{CPM}} = \frac{\kappa_{\mathrm{av}}}{LS_{\mathrm{av}}}\frac{\Delta T}{T_{\mathrm{m}}}\left(-1 + \sqrt{1 + zT_{\mathrm{m}}}\right) \quad , \tag{16}$$

where $\Delta T = T_{\mathrm{a}} - T_{\mathrm{s}}$, $T_{\mathrm{m}} = (T_{\mathrm{a}} + T_{\mathrm{s}})/2$, and $z = (S_{\mathrm{av}}^2\,\sigma_{\mathrm{av}})/\kappa_{\mathrm{av}}$ are the respective temperature difference, the (arithmetic) average temperature, and the material's figure of merit. Setting these optimum current densities in Eq. (14) and Eq. (15), respectively, leads directly to the well-known formulae of maximum performance parameters:

$$p_{\mathrm{net,max}}^{\mathrm{CPM}} = S_{\mathrm{av}}^2\sigma_{\mathrm{av}}\frac{(\Delta T)^2}{4L} \quad \text{and} \quad \eta_{\mathrm{max}}^{\mathrm{CPM}} = \frac{\Delta T}{T_{\mathrm{a}}}\frac{\sqrt{1 + zT_{\mathrm{m}}} - 1}{\sqrt{1 + zT_{\mathrm{m}}} + T_{\mathrm{s}}/T_{\mathrm{a}}} \quad , \tag{17}$$

see, e.g., Refs. 7–9. Note that these formulae are in a strict sense only valid for constant material properties, although they are often used as an approximation for temperature dependent materials. For those materials the usage of an effective figure of merit is supposed, especially for large temperature differences ΔT. [6,29,66–70]

V. TEG PERFORMANCE OPTIMIZATION VIA LINEAR GRADING

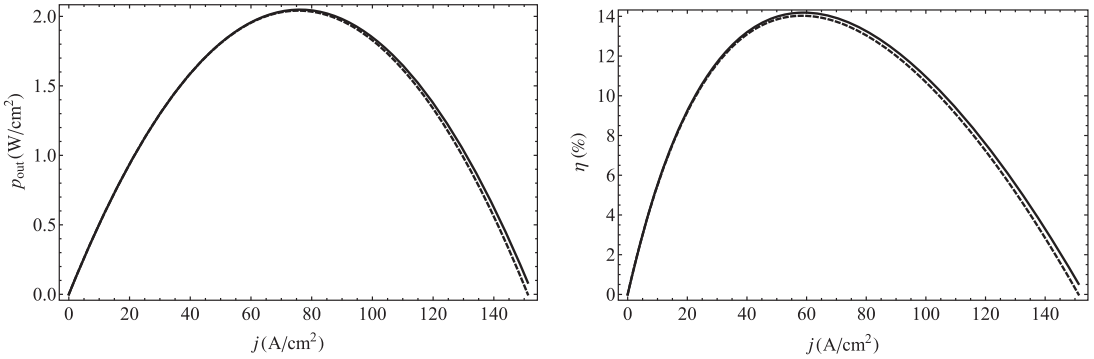
It is not the aim of this paper to discuss all optimization variants based on given linear profiles. In general, it is possible to search for the global maximum and the related optimum current of the performance parameter under consideration by adjusting the slope of the material profile via the ratios ξ_κ, ξ_S, and ξ_σ with respective fixed spatial averages κ_{av}, S_{av}, and σ_{av}.

Considering the net power output density first, we find Eq. (18) for a constant electrical conductivity ($\xi_\sigma = 1$), which is supposed to be in the vicinity of the maximal performance, after integration by parts[71]:

$$p_{\mathrm{net}} \equiv p_{\mathrm{net}}(j, \xi_S, \xi_\kappa) = -\frac{j^2L}{\sigma_{\mathrm{av}}} - j\frac{2S_{\mathrm{av}}}{1 + \xi_S}\left[T_{\mathrm{s}} - T_{\mathrm{a}}\xi_S - \frac{(1 - \xi_S)}{L}\int_0^L T(x)dx\right]. \tag{18}$$

In Eq. (18) the grading of ξ_κ enters through the spatial average $L^{-1}\int_0^L T(x)dx$. The efficiency can be calculated with Eqs. (12), (18), and (1b).

https://doi.org/10.1557/jmr.2011.91 Published online by Cambridge University Press



(a) $p_{\mathrm{net}}^{\mathrm{CPM}}(j)$ (dashed) and $p_{\mathrm{net}}^{\mathrm{LPM}}(j)$ (solid) **(b)** $\eta^{\mathrm{CPM}}(j)$ (dashed) and $\eta^{\mathrm{LPM}}(j)$ (solid)

FIG. 3. Comparison of power output density and efficiency of a CPM, i.e., totally homogeneous, and LPM (graded) element for a TEG element (L = 5 mm, T_a = 600 K, T_s = 300 K, S_{av} = 180 μV/K, κ_{av} = 1.35 W/m K, $\sigma_{av} = 14 \cdot 10^4$ S/m) depending on the electrical current density for the optimal parameters $\xi_{S,\mathrm{opt}}$ given in Table I.

TABLE I. Special cases I.

Quantity	Expression
	$\kappa(x) = \kappa_{av}$, $\sigma(x) = \sigma_{av}$, $S(x) = S_{av}$, or $\xi_\kappa = \xi_\sigma = \xi_S = 1$
Profile:	$T(x) = T_a + \Delta T \frac{x}{L} + A_1 x(L-x)$
Derivative:	$T'(x) = \frac{\Delta T}{L} + A_1(L-2x)$
Spatial average:	$\frac{1}{L}\int_0^L T(x)dx = \frac{T_a+T_s}{2} + A_1\frac{L^2}{6}$
	$\kappa(x) = \kappa_{av}$, $\sigma(x) = \sigma_{av}$, or $\xi_\kappa = \xi_\sigma = 1$
Profile:	$T(x) = \frac{\sin(A_2 x)}{\sin(A_2 L)}\{T_s - T_a\cos(A_2 L) + A_3[\cos(A_2 L) - 1]\} + T_a\cos(A_2 x) - A_3[\cos(A_2 x) - 1]$
Derivative:	$T'(x) = A_2\left[\frac{\cos(A_2 x)}{\sin(A_2 L)}\{T_s - T_a\cos(A_2 L) + A_3[\cos(A_2 L) - 1]\} + (A_3 - T_a)\sin(A_2 x)\right]$
Spatial average:	$\frac{1}{L}\int_0^L T(x)d = \frac{1}{A_2 L}\left[\frac{1-\cos(A_2 L)}{\sin(A_2 L)}\{T_s - T_a\cos(A_2 L) + A_3[\cos(A_2 L) - 1]\} + (T_a - A_3)\sin(A_2 L)\right] + A_3$
	$\kappa(x) = \kappa_{av}$, $S(x) = S_{av}$, or $\xi_\kappa = \xi_S = 1$
Profile:	$T(x) = T_a + \Delta T\frac{x}{L} + A_1 L^2\frac{(1+\xi_\sigma)}{(1-\xi_\sigma)^2}\{(1-\frac{x}{L})\xi_\sigma \ln\xi_\sigma - [\xi_\sigma + (1-\xi_\sigma)\frac{x}{L}]\ln[\xi_\sigma + (1-\xi_\sigma)\frac{x}{L}]\}$
Derivative:	$T'(x) = \frac{\Delta T}{L} - A_1 L\frac{(1+\xi_\sigma)}{(1-\xi_\sigma)^2}\{\xi_\sigma \ln\xi_\sigma + (1-\xi_\sigma)(\ln[\xi_\sigma + (1-\xi_\sigma)\frac{x}{L}] + 1)\}$
Spatial average:	$\frac{1}{L}\int_0^L T(x)dx = \frac{T_a+T_s}{2} + A_1\frac{L^2}{2}\frac{(1+\xi_\sigma)}{(1-\xi_\sigma)^2}\left\{\xi_\sigma \ln\xi_\sigma + \frac{1}{1-\xi_\sigma}[\frac{1}{2} + \xi_\sigma^2(\ln\xi_\sigma - \frac{1}{2})]\right\}$
	$\sigma(x) = \sigma_{av}$, $S(x) = S_{av}$, or $\xi_\sigma = \xi_S = 1$
Profile:	$T(x) = T_s - \frac{\ln(\xi_\kappa + (1-\xi_\kappa)\frac{x}{L})}{\ln\xi_\kappa}\Delta T + A_1 L^2\frac{(1+\xi_\kappa)}{(1-\xi_\kappa)}\left[(1-\frac{x}{L}) - \frac{\ln(\xi_\kappa + (1-\xi_\kappa)\frac{x}{L})}{\ln\xi_\kappa}\right]$
Derivative:	$T'(x) = -\frac{\Delta T}{L}\frac{(1-\xi_\kappa)}{\ln\xi_\kappa}\frac{1}{\xi_\kappa + (1-\xi_\kappa)\frac{x}{L}} - A_1 L\frac{(1+\xi_\kappa)}{(1-\xi_\kappa)}\left[1 + \frac{1}{\xi_\kappa + (1-\xi_\kappa)\frac{x}{L}}\frac{(1-\xi_\kappa)}{\ln\xi_\kappa}\right]$
Spatial average:	$\frac{1}{L}\int_0^L T(x)dx = T_s - \frac{\Delta T}{(1-\xi_\kappa)\ln\xi_\kappa}\{-1 + \xi_\kappa(1-\ln\xi_\kappa)\} + A_1 L^2\frac{(1+\xi_\kappa)}{(1-\xi_\kappa)}\left[\frac{1}{2} - \frac{1}{(1-\xi_\kappa)\ln\xi_\kappa}\{-1 + \xi_\kappa(1-\ln\xi_\kappa)\}\right]$
Shortcuts:	$\Delta T = T_s - T_a$, $A_1 = \frac{j^2}{2\kappa_{av}\sigma_{av}}$, $A_2 = \sqrt{-\frac{jb(S)}{\kappa_{av}}}$, $A_3 = \frac{j}{\sigma_{av}b(S)}$, $b(S) = \frac{\Delta S}{L}$

We first discuss the particular case of having only one linear profile for the Seebeck coefficient, where as the conductivities are supposed to be constant ($\xi_S \neq 1$, $\xi_\kappa = \xi_\sigma = 1$). For that the material parameters are chosen as S_{av} = 180 μV/K, κ_{av} = 1.35 W/m K, and $\sigma_{av} = 14 \cdot 10^4$ S/m exemplarily; and the dimensionless figure of merit is approximately 1 at T = 300 K. For all numerical calculations we suppose an element length L = 5 mm and the boundary temperatures are fixed to T_a = 600 K and T_s = 300 K, i.e., a temperature difference ΔT = 300 K. In the CPM case the optimal performance parameters $p_{\mathrm{net,max}}^{\mathrm{CPM}}$, $\eta_{\mathrm{max}}^{\mathrm{CPM}}$, as well as the optimal current densities are given by Eqs. (16) and (17), whereas for LPM one ends up in a multidimensional extreme value task with a system of equations leading to the optimum current densities j_{opt} and grading parameters ξ_{opt}, e.g.,

$$\frac{\partial p_{\mathrm{net}}(j,\xi_S,\xi_\kappa)}{\partial j} = 0 \quad , \quad \frac{\partial p_{\mathrm{net}}(j,\xi_S,\xi_\kappa)}{\partial \xi_S} = 0 \quad , \quad \text{and} \quad \frac{\partial p_{\mathrm{net}}(j,\xi_S,\xi_\kappa)}{\partial \xi_\kappa} = 0 \quad .$$

By linear profiles of S both the power output and the efficiency can be increased. As for CPM the optimal

https://doi.org/10.1557/jmr.2011.91 Published online by Cambridge University Press

TABLE II. Spacial cases II.

Quantity	Expression
	$\sigma(x) = \sigma_{av}$ or $\xi_\sigma = 1$
Profile:	$T(x) = C_1 \mathrm{J}_0\left(A_4\sqrt{\kappa(x)}\right) + C_2 \mathrm{Y}_0\left(A_4\sqrt{\kappa(x)}\right) + \frac{j}{b(S)\sigma_{av}}$
Derivative:	$T'(x) = -\frac{A_4 b(\kappa)}{2\sqrt{\kappa(x)}}\left\{C_1 \mathrm{J}_1\left(A_4\sqrt{\kappa(x)}\right) + C_2 \mathrm{Y}_1\left(A_4\sqrt{\kappa(x)}\right)\right\}$
Spatial average:	$\frac{1}{L}\int_0^L T(x)dx = \frac{j}{b(S)\sigma_{av}} + \frac{2}{A_4 L b(\kappa)}\left[C_1(\sqrt{\kappa_s}\mathrm{J}_{1s} - \sqrt{\kappa_a}\mathrm{J}_{1a}) + C_2(\sqrt{\kappa_s}\mathrm{Y}_{1s} - \sqrt{\kappa_a}\mathrm{Y}_{1a})\right]$
Constants:	$C_1 = \frac{\left\{T_s \mathrm{Y}_{0a} - T_a \mathrm{Y}_{0s} + \frac{j(\mathrm{Y}_{0s} - \mathrm{Y}_{0a})}{b(S)\sigma_{av}}\right\}}{(\mathrm{Y}_{0a}\mathrm{J}_{0s} - \mathrm{Y}_{0s}\mathrm{J}_{0a})}, C_2 = \frac{\left\{T_a \mathrm{J}_{0s} - T_s \mathrm{J}_{0a} + \frac{j(\mathrm{J}_{0a} - \mathrm{J}_{0s})}{b(S)\sigma_{av}}\right\}}{(\mathrm{Y}_{0a}\mathrm{J}_{0s} - \mathrm{Y}_{0s}\mathrm{J}_{0a})},$
	$\mathrm{Y}_{0a} = \mathrm{Y}_0\left(A_4\sqrt{\kappa(0)}\right) = \mathrm{Y}_0\left(A_4\sqrt{\kappa_a}\right),\ \mathrm{Y}_{0s} = \mathrm{Y}_0\left(A_4\sqrt{\kappa_s}\right),\ \mathrm{J}_{0a} = \mathrm{J}_0\left(A_4\sqrt{\kappa_a}\right),\ \mathrm{J}_{0s} = \mathrm{J}_0\left(A_4\sqrt{\kappa_s}\right)$
	$\mathrm{Y}_{1a} = \mathrm{Y}_1\left(A_4\sqrt{\kappa(0)}\right) = \mathrm{Y}_1\left(A_4\sqrt{\kappa_a}\right), \mathrm{Y}_{1s} = \mathrm{Y}_1\left(A_4\sqrt{\kappa_s}\right), \mathrm{J}_{1a} = \mathrm{J}_1\left(A_4\sqrt{\kappa_a}\right), \mathrm{J}_{1s} = \mathrm{J}_1\left(A_4\sqrt{\kappa_s}\right)$
	$S(x) = S_{av}$ or $\xi_S = 1$
Profile:	$T(x) = T_s + A_5\left\{\mathrm{Li}_2(A_6) - \mathrm{Li}_2\left(1 - A_6\frac{\sigma(x)}{\sigma_s}\right) - \ln\left(\frac{\sigma(x)}{\sigma_s}\right)\ln\left(1 + A_7\frac{\kappa(x)}{\kappa_s}\right)\right\} + \frac{\ln\left(\frac{\kappa(x)}{\kappa_s}\right)}{\ln\xi_\kappa}A_9$
Derivative:	$T'(x) = -A_5\left\{\frac{A_6(1-\xi_\sigma)}{L}\frac{\ln\left(A_6\frac{\sigma(x)}{\sigma_s}\right)}{1 - A_6\frac{\sigma(x)}{\sigma_s}} + \frac{(1-\xi_\sigma)}{L}\frac{\sigma_s}{\sigma(x)}\ln\left(1 + A_7\frac{\kappa(x)}{\kappa_s}\right) + \frac{A_7(1-\xi_\kappa)}{L}\frac{\kappa_s}{\kappa(x)}\ln\left(\frac{\sigma(x)}{\sigma_s}\right)\right\} + A_9\frac{1-\xi_\kappa}{L\ln\xi_\kappa}\frac{\kappa_s}{\kappa(x)}$
Spatial average:	$\frac{1}{L}\int_0^L T(x)dx = T_s + A_9\frac{\xi_\kappa(1-\ln\xi_\kappa)-1}{\ln\xi_\kappa(1-\xi_\kappa)} + A_5\left\{\mathrm{Li}_2(A_6) + \frac{1}{\xi_\sigma - 1}\left[\mathrm{Li}_2(A_7) + \frac{1-\xi_\sigma}{1-\xi_\kappa}(\ln A_7 - 1) - \xi_\sigma \mathrm{Li}_2(A_7\xi_\kappa)\right.\right.$
	$\left. + \frac{\xi_\kappa(1-\xi_\sigma)}{\xi_\kappa - 1}(\ln(A_7\xi_\kappa) - 1)\right] - \left[\ln(1 + A_7) - 2 + \frac{\xi_\sigma}{1-\xi_\sigma}\left(\mathrm{Li}_2\left(\frac{1+A_7}{2}\right) - \mathrm{Li}_2\left(\frac{1+A_7\xi_\kappa}{2}\right) - \ln\xi_\sigma(1 - \ln 2)\right)\right.$
	$\left.\left. + \frac{1/A_7 + \xi_\kappa}{\xi_\kappa - 1}\left(\mathrm{Li}_2\left(\frac{1+A_7}{2}\right) - \mathrm{Li}_2\left(\frac{1+A_7\xi_\kappa}{2}\right) + \ln\left(\frac{1+A_7\xi_\kappa}{1+A_7}\right) + \ln\xi_\sigma \ln\left(\frac{1+A_7\xi_\kappa}{2}\right)\right)\right]\right\}$
Shortcuts:	$\frac{\kappa(x)}{\kappa_s} = \xi_\kappa + (1 - \xi_\kappa)\frac{x}{L}, \frac{\sigma(x)}{\sigma_s} = \xi_\sigma + (1 - \xi_\sigma)\frac{x}{L}, A_9 = \Delta T - A_5[\mathrm{Li}_2(A_6) - \mathrm{Li}_2(A_6\xi_\sigma) - \ln\xi_\sigma \ln(A_7\xi_\kappa)]$
Shortcuts:	$b(y) = \frac{\Delta y}{L}(y = \kappa, \sigma, S), A_2 = \sqrt{-\frac{jb(S)}{\kappa_{av}}}, A_4 = -2\sqrt{\frac{-jb(S)}{b^2(\kappa)}}, A_5 = \frac{j^2}{b(\kappa)b(\sigma)}, A_6 = \frac{\xi_\kappa - 1}{\xi_\kappa - \xi_\sigma}, A_7 = \frac{1-\xi_\sigma}{\xi_\kappa - \xi_\sigma}, A_8 = \frac{1}{b(\sigma)}\sqrt{-\frac{j}{\kappa_{av}b(S)}}$

TABLE III. Spacial cases III.

Quantity	Expression
	$\kappa(x) = \kappa_{av}$ or $\xi_\kappa = 1$
Profile:	$T(x) = C_1\cos(A_2x) + C_2\sin(A_2x) - jA_8\{\mathrm{Si}[f(x)]\cos[f(x)] - \mathrm{Ci}[-f(x)]\sin[f(x)]\}$
Derivative:	$\frac{T'(x)}{A_2} = -C_1\sin(A_2x) + C_2\cos(A_2x) - jA_8\left\{\sin(f(x))\left[\mathrm{Si}(f(x)) - \frac{\cos(f(x))}{f(x)}\right] - \cos(f(x))\left[\mathrm{Ci}(-f(x)) + \frac{\sin(f(x))}{f(x)}\right]\right\}$
Spatial average:	$\frac{A_2}{L}\int_0^L T(x)dx = \frac{C_1}{L}\sin(A_2L) + \frac{C_2}{L}[1 - \cos(A_2L)] - \frac{jA_8}{L}[\mathrm{Si}(f_a)\sin(f_a) - \mathrm{Si}(f_s)\sin(f_s)$
	$+ \mathrm{Ci}(-f_s)\cos(-f_s) - \mathrm{Ci}(-f_a)\cos(-f_a) + \mathrm{Ci}(2f_a) - \mathrm{Ci}(2f_s)]$
Constants:	$C_1 = T_a + jA_8\{\mathrm{Si}[f_a]\cos[f_a] - \mathrm{Ci}[-f_a]\sin[f_a]\}$
	$C_2 = \frac{1}{\sin(A_2L)}[T_s + jA_8\{\mathrm{Si}[f_s]\cos[f_s] - \mathrm{Ci}[-f_s]\sin[f_s]\}] - C_1\cot(A_2L)$
	$f(x) \equiv f(x; L, \xi_\sigma) = A_2\left(\frac{L\xi_\sigma}{\xi_\sigma - 1} - x\right), f_a \equiv f(x = 0) = A_2\frac{L\xi_\sigma}{\xi_\sigma - 1}, f_s \equiv f(x = L) = \frac{A_2L}{\xi_\sigma - 1}$

parameters are different depending on what has to be optimized, p_{net} or η, but we find the same directions in the optimization strategy. Both TEG performance parameters are displayed in Fig. 3 for a TE element of length L = 5 mm and a fixed temperature difference ΔT = 300K, showing by that the difference between homogeneous and graded material. The results for CPM (i.e., totally homogeneous) and LPM (i.e., linear material profiles) are also compared in Table IV. Using Eqs. (14) and (18) the difference between the power output in the CPM and LPM case can easily be deduced to

$$\delta p_{net} = p_{net}(j, \xi_S) - p_{net}^{CPM}(j) = j\Delta S[T_{av} - T_m] \quad , \quad (19)$$

with mean temperature $T_m = (1/2)(T_a + T_s)$ and averaged temperature $T_{av} = (1/L)\int_0^L T(x)dx$. It is clearly visible from Eq. (19) that two factors have influence on the difference δp_{net}; one factor is the slope of the Seebeck coefficient $b(S) = \Delta S/L$. Note that we have $\Delta S = 0$ in the CPM case and hence a zero difference. A second factor is the deviation of the temperature profile $T(x)$ from a pure

https://doi.org/10.1557/jmr.2011.91 Published online by Cambridge University Press

TABLE IV. Values of the optimum performance parameters for the given material.

	Maximum output power output density			Maximum efficiency		
	$j_{opt,p}$ (A/cm^2)	$\xi_{S,opt}$	$p_{net,max}$ (W/cm^2)	$j_{opt,\eta}$ (A/cm^2)	$\xi_{S,opt}$	η_{max}(%)
CPM	75.6	1	2.041	58.5	1	14.03
LPM	76.1	0.85	2.048	59.0	0.67	14.19

linear one. Linear material profiles lead clearly to a nonlinear temperature profile, shifting the spatial average away from the mean of the boundary temperatures and leading to an increasing difference in power output.

Table IV clarifies that graded materials design may imply only a small reserve to improve the performance of a TEG if a constant thermal conductivity is assumed (see also Ref. 65). The increase of TEG's power output and efficiency is more pronounced when considering linear profiles $S(x)$ and $\kappa(x)$ as a further example. The first results were published in Ref. 71, demonstrating the ability to exactly evaluate the limiting cases for extreme parameters ξ_S and ξ_κ.

VI. CONCLUSIONS

In the present paper we studied transport processes in a continuous medium with local equilibrium. In particular, the paper focused on TE effects as phenomena associated with the simultaneous presence of an electric current and a heat flux. Whereas in the conventional thermodynamics of irreversible processes the transport coefficients are assumed to be at least piecewise constant, we discussed here the case that the TE material parameters offers a spatial dependence. Such a situation is realized in graded and segmented TE elements. In order to optimize the performance of TE elements it is appropriate to search for analytical solutions of the underlying equations. Here we discussed the thermal energy balance in the steady state that results in a linear differential equation of the temperature distribution $T(x)$ when assuming linear varying spatial material parameters in a 1D setup. For this case, we attained the analytical solution in terms of Bessel functions. From here the performance parameters like the electrical power and the efficiency of a graded TEG of fixed length under appropriate boundary conditions are specified exemplarily.

The importance of FGM research to device optimization has appeared particularly attractive for TEGs, because maximum power and maximum efficiency points are close together. The question whether compromise gradient schemes can be found is therefore of importance for the practice. There is hope that the knowledge of optimized linear, spatial profiles will provide a chance to come closer to the optimal material gradients. Of course, it would be beneficial to use the results of the LPM approach for the calculation of real FGM and segmented materials and compare it with experimental results already reported in the literature. However, as the CPM, the LPM is not suitable for a direct comparison to the experiment, especially when operating under great temperature differences. The investigation here should only give qualitative hints about how to do the grading knowing that it is not possible to have the TE material properties all at once linear because the interrelation between them is rather nontrivial. In the experiments there is a concentration on the determination of the temperature dependence of the material properties, because this dependence is unique for a material whereas a position dependence is connected with a particular sample (shape, topology). For an overview of experiments in FGM research, see, e.g., Refs. 5, 6, 29, and 72–77. There are few experiments concerning the spatially resolved measurement of TE material properties such as the potential scanning microscope (see, e.g., Refs. 78 and 79). Until now the progress in the material science of TE elements has been mainly attributable to simulations and modeling using different numerical methods such as the finite difference method or finite element method; see, e.g., Refs. 29, 36–40, 62, and 80–96. Of course, an analytical solution can also be used for testing numerical methods.

ACKNOWLEDGMENTS

The authors are very grateful to G.J. Snyder, California Institute of Technology, and C. Goupil, Laboratoire CRISMAT, Caen, France, for helpful discussions.

REFERENCES

1. K. Behnia, D. Jaccard, and J. Flouquet: On the thermoelectricity of correlated electrons in the zero-temperature limit. *J. Phys. Condens. Matter* **16**, 5187 (2004).
2. K. Behnia: The Nernst effect and the boundaries of the Fermi liquid picture. *J. Phys. Condens. Matter* **21**, 113101 (2009).
3. A.A. Kovalev and Y. Tserkovnyak: Thermoelectric spin transfer in textured magnets. *Phys. Rev. B* **80**, 100408 (2009).
4. L. Zhu, R. Ma, L. Sheng, M. Liu, and D.-N. Sheng: Universal thermoelectric effect of dirac fermions in graphene. *Phys. Rev. Lett.* **104**, 076804 (2010).
5. V.L. Kuznetsov: Functionally graded materials for thermoelectric applications, in *CRC Handbook of Thermoelectrics: Macro to Nano* (Taylor & Francis, Boca Raton, FL, 2006; chap. 28).
6. E. Müller, K. Zabrocki, C. Goupil, G.J. Snyder, and W. Seifert: Functionally graded thermoelectric generator and cooler elements. in *CRC Handbook of Thermoelectrics: Thermoelectrics and Its Energy Harvesting* (D.M. Rowe, ed., RC, Boca Raton, FL, 2011).
7. E. Altenkirch: Über den Nutzeffekt der Thermosäulen. *Phys. Z.* **10**, 560–580, (1909).

https://doi.org/10.1557/jmr.2011.91 Published online by Cambridge University Press

8. E. Altenkirch: Elektrothermische Kälteerzeugung und reversible elektrische Heizung. *Phys. Z.* **12**, 920–924 (1911).
9. A.F. Ioffe: *Semiconductor Thermoelements and Thermoelectric Cooling* (Infosearch, Ltd., London, 1957).
10. M. Jonson and G.D. Mahan: Mott's formula for the thermopower and the Wiedemann–Franz law. *Phys. Rev. B* **21**, 4223–4229 (1980).
11. G. Wiedemann and R. Franz: Ueber die Wärme-Leitungsfähigkeit der Metalle. *Ann. Phys.* **89**, 497–531 (1953).
12. N.W. Ashcroft and N.D. Mermin: *Solid State Physics* (Saunders College, Philadelphia, PA, 1976).
13. M. Telkes: Westinghouse Research Report R-94264-B (1938).
14. C. Wood: Materials for thermoelectric energy conversion. *Reports Progr. Phys.* **51**, 459–539 (1988).
15. M. Telkes: The efficiency of thermoelectric generators. I. *J. Appl. Phys.* **18**, 1116–1127 (1947).
16. M. Telkes: Solar thermoelectric generators. *J. Appl. Phys.* **25**, 765–777 (1954).
17. M. Telkes: Power output of thermoelectric generators. *J. Appl. Phys.* **25**, 1058–1059 (1954).
18. L. Onsager: Reciprocal relations in irreversible processes. I. *Phys. Rev.* **37**, 405–426 (1931).
19. L. Onsager: Reciprocal relations in irreversible processes. II. *Phys. Rev.* **38**, 2265–2279 (1931).
20. H.J. Goldsmid and R.W. Douglas: The use of semiconductors in thermoelectric refrigeration. *Br. J. Appl. Phys.* **5**, 386 (1954).
21. D.M. Rowe, ed.: *CRC Handbook of Thermoelectrics* (RC, Boca Raton, FL, 1995).
22. D.M. Rowe, ed.: *CRC Handbook of Thermoelectrics: Macro to Nano*. (RC, Boca Raton, FL, 2006).
23. S.D. Riffat and Xi. Ma: Irreversible thermodynamics of thermoelectricity. *Appl. Therm. Eng.* **23**, 913–935 (2003).
24. C.B. Vining: An inconvenient truth about thermoelectrics. *Nature Mater.* **8**, 83–85 (2009).
25. I. Shiota and Y. Miyamoto, ed.: Functionally graded material 1996, in *Proceedings of the 4th International Symposium on Functionally Graded Materials* (Elsevier, New York, 1996).
26. T.M. Tritt, ed.: *Recent Trends in Thermoelectric Materials Research III. Vol 71: Semiconductors and Semimetals* (Academic Press, San Diego, CA, 2001).
27. C.A. Domenicali: Irreversible thermodynamics of thermoelectric effects in inhomogeneous, anisotropic media. *Phys. Rev.* **92**, 877–881 (1953).
28. C.A. Domenicali: Irreversible thermodynamics of thermoelectricity. *Rev. Mod. Phys.* **26**, 237–275 (1954).
29. A.E. Kaliazin, V.L. Kuznetsov, and D.M. Rowe: Rigorous calculations related to functionally graded and segmented thermoelements. In *Proceedings ICT 2001. Twentieth International Conference on Thermoelectrics* (IEEE, 2001; pp. 286–292).
30. J.H. Lienhard, IV and J.H. Lienhard, V: *A Heat Transfer Textbook* (3rd ed.; Phlogiston Press, Cambridge, MA, 2008).
31. J. Schilz, E. Müller, L. Helmers, Y.S. Kang, Y. Noda, and M. Niino: On the composition function of graded thermoelectric materials. *Mater. Sci. Forum* **308–311**, 647–652 (1999).
32. P.H. Egli: *Thermoelectricity* (John Wiley & Sons, Inc., New York, 1960).
33. D.K.C. MacDonald: *Thermoelectricity: An Introduction to the Principles* (Dover Publications, Inc., New York, 2006).
34. L.J. Ybarrondo: Effects of surface heat transfer and spatial property dependence on the optimum performance of a thermoelectric heat pump. Ph.D. Thesis, Georgia Institute of Technology, Atlanta, GA, 1964).
35. L.J. Ybarrondo and J.E. Sunderland: Influence of spatially dependent properties on the performance of a thermoelectric heat pump. *Adv. Energy Convers.* **5**, 383–405 (1965).
36. E. Müller, S. Walczak, W. Seifert, C. Stiewe, and G. Karpinski: Numerical performance estimation of segmented thermoelectric elements. In *ICT 2005—24th International. Conference. on Thermoelectrics* (T.M. Tritt, ed.; Institute of Electrical and Electronics Engineers, Inc., New York, 2005; pp. 352–357).
37. W. Seifert, E. Müller, and S. Walczak: Generalized analytic description of one dimensional non-homogeneous TE cooler and generator elements based on the compatibility approach. In *25th International Conference on Thermoelectrics* (P. Rogl, ed.; IEEE, Piscataway, NJ, 2006; pp. 714–719).
38. E. Müller, G. Karpinski, L.M. Wu, S. Walczak, and W. Seifert: Separated effect of 1d thermoelectric material gradients. In *25th International Conference on Thermoelectrics* (P. Rogl, ed.; IEEE, Piscataway, NJ, 2006; pp. 201–209).
39. Z. Bian and A. Shakouri: Beating the maximum cooling limit with graded thermoelectric materials. *Appl. Phys. Lett.* **89**, 212101 (2006).
40. Z. Bian, H. Wang, Q. Zhou, and A. Shakouri: Maximum cooling temperature and uniform efficiency criterion for inhomogeneous thermoelectric materials. *Phys. Rev. B Condens. Matter Mater. Phys.* **75**, 245208 (2007).
41. G.J. Snyder: Thermoelectric power generation: Efficiency and compatibility. In *CRC Handbook of Thermoelectrics: Macro to Nano* (D.M. Rowe, ed.; Taylor & Francis, Boca Raton, FL, 2006; chap. 9).
42. W. Seifert, E. Müller, G.J. Snyder, and S. Walczak: Compatibility factor for the power output of a thermogenerator. *Phys. Status Solidi*: **1**, 250–252 (2007).
43. O.S. Gryaznov, B.Ya. Moizhes, and V.A. Nemchinskii: Generalized thermoelectric efficiency. *Soviet Phys. Techn. Phys.* **23**, 975–980 (1978).
44. S. de Groot and P. Mazur: *Non-Equilibrium Thermodynamics* (Dover, London, 1984).
45. C.A. Domenicali: Stationary temperature distribution in an electrically heated conductor. *J. Appl. Phys.* **25**, 1310–1311 (1954).
46. G.D. Mahan: Density variations in thermoelectrics. *J. Appl. Phys.* **87**, 7326–7332 (2000).
47. L. Onsager: Theories and problems of liquid diffusion. *Annals. NY Acad. Sci.* **46**, 241–265 (1945).
48. S.R. de Groot: *Thermodynamics of Irreversible Processes* (North-Holland Publishing Company, Amstemdam, 1963).
49. H.B. Callen: On the theory of irreversible processes. Ph.D. Thesis, MIT, Cambridge, MA, 1947.
50. H.B. Callen: The application of Onsager's reciprocal relations to thermoelectric, thermomagnetic, and galvanomagnetic effects. *Phys. Rev.* **73**, 1349–1358 (1948).
51. W. Seifert, M. Ueltzen, and E. Müller: One-dimensional modelling of thermoelectric cooling. *Phys. Status Solidi A* **1**(194), 277–290 (2002).
52. G.D. Mahan: Inhomogeneous thermoelectrics. *J. Appl. Phys.* **70**, 4551–4554 (1991).
53. T.C. Harman and J.M. Honig: *Thermoelectric and Thermomagnetic Effects and Applications* (McGraw–Hill Book Company, New York, 1967).
54. R.J. Buist: The extrinsic Thomson effect. In *Proceedings of the 14th International Conference on Thermoelectrics*, edited by M.V. Vedernikov (A.F. Ioffe Physical-Technical Institute, St. Petersburg, Russia, 1995; pp. 301–304).
55. W. Seifert, E. Müller, and S. Walczak: Local optimization strategy based on first principles of thermoelectrics. *Phys. Status Solidi A* **205**(12), 2908–2918 (2008).
56. M. Abramowitz and I.A. Stegun, ed.: *Handbook of Mathematical Functions with Formulas, Graphs, and Mathematical Tables*, 10th ed. (Dover Publications, Inc., New York, 1972).

https://doi.org/10.1557/jmr.2011.91 Published online by Cambridge University Press

57. N.N. Lebedev and R.A. Silverman: *Special Functions and Their Applications* (Dover Publications, Inc., New York, 1972).
58. O.J. Farrell and B. Ross: *Solved Problems in Analysis: As Applied to Gamma, Beta, Legendre and Bessel Functions* (Dover Publications, Inc., New York, 1971).
59. F. Bowman: *Introduction to Bessel Functions* (Dover Publications, Inc., New York, 1958).
60. G.B. Mathews and E. Meissel: *A Treatise on Bessel Functions and Their Applications to Physics* (BiblioBazaar, LLC, Charleston, SC, 2008).
61. R. Ure and R. Heikes: The figure of merit of a thermoelectric generator. *Adv. Energy Convers.* **2**, 177 (1962).
62. L. Helmers, E. Müller, J. Schilz, and W.A. Kaysser: Graded and stacked thermoelectric generators—Numerical description and maximisation of output power. *Mater. Sci. Eng. B* **56**, 60–68 (1998).
63. T.S. Ursell and G.J. Snyder: Compatibility of segmented thermoelectric generators. In *Twenty-First International Conference on Thermoelectrics*, edited by Thierry Caillat/G. Jeffrey Snyder (IEEE, 2002; pp. 412–417).
64. G.J. Snyder: Application of the compatibility factor to the design of segmented and cascaded thermoelectric generators. *Appl. Phys. Lett.* **84**, 2436–2438 (2004).
65. W. Seifert, K. Zabrocki, G.J. Snyder, and E. Müller: Power-related compatibility and maximum electrical power output of a thermogenerator. *Phys. Status. Solidi A* **207**, 2399–2406 (2010).
66. B.Ya Moizhes: The influence of the temperature dependence of physical parameters on the efficiency of thermoelectric generators and refrigerators. *Sov. Phys. Solid State* **2**, 728–737 (1960).
67. J.M. Borrego: Carrier concentration optimization in semiconductor thermoelements. *IEEE Trans. Electron Devices* **10**, 364–370 (1963).
68. J.M. Borrego: Approximate analysis of the operation of thermoelectric generators with temperature dependent parameters. *IEEE Trans. Aerospace* **2**, 4–9 (1964).
69. A.A. Efremov and A.S. Pushkars: Energy calculation of thermoelements with arbitrary temperature dependence of thermoelectric properties of materials by heat balance technique. *Energy Convers.* **11**, 101–104 (1971).
70. A. Muto, D. Kraemer, Q. Hao, Z.F. Ren, and G. Chen: Thermoelectric properties and efficiency measurements under large temperature differences. *Rev. Sci. Instrum.* **80**, 093901 (2009).
71. K. Zabrocki, E. Müller, and W. Seifert: One-dimensional modeling of thermogenerator elements with linear material profiles. *J. Electron. Mater.* **39**, 1724–1729 (2010).
72. V.L. Kuznetsov, L.A. Kuznetsova, A.E. Kaliazin, and D.M. Rowe: High performance functionally graded and segmented Bi_2Te_3-based materials for thermoelectric power generation. *J. Mater. Sci.* **37**, 2893–2897 (2002).
73. V.L. Kuznetsov and P.P. Edwards: Functional materials for sustainable energy technologies: Four case studies. *ChemSus Chem* **3**, 44–58 (2010).
74. Z. Dashevsky, S. Shusterman, M.P. Dariel, and I. Drabkin: Thermoelectric efficiency in graded indium-doped PbTe crystals. *J. Appl. Phys.* **92**, 1425–1430 (2002).
75. Z. Dashevsky, Y. Gelbstein, I. Edry, I. Drabkin, and M.P. Dariel: Optimization of thermoelectric efficiency in graded materials. In *Proceedings of the 22nd International Conference on Thermoelectrics*, edited by H. Scherrer and J.-C. Tedenac (IEEE, 2003; pp. 421–424).
76. Y. Gelbstein, Z. Dashevsky, and M.P. Dariel. High performance n-type PbTe-based materials for thermoelectric applications. *Phys. B Condens. Matter* **363**(1–4), 196–205 (2005).
77. E. Müller, Č. Drašar, J. Schilz, and W.A. Kaysser: Functionally graded materials for sensor and energy applications. *Mater. Sci. Eng. A* **362**, 17–39 (2003).
78. P. Ziolkowski, G. Karpinski, D. Platzek, C. Stiewe, and E. Müller: Application overview of the potential Seebeck microscope. In *25th International Conference of Thermoelectrics 06* (P. Rogl, ed.; 2006; pp. 684–688).
79. D. Platzek, G. Karpinski, C. Drasar, and E. Müller: Seebeck scanning microprobe for thermoelectric FGM. *Mater. Sci. Forum* **492–493**, 587–592 (2005).
80. B. Sherman, R.R. Heikes, and R.W. Ure, Jr.: Calculation of efficiency of thermoelectric devices. *J. Appl. Phys.* **31**, 1–16 (1960).
81. B. Sherman, R.R. Heikes, and R.W. Ure, Jr.: Calculation of efficiency of thermoelectric devices. In *Thermoelectric Materials and Devices* (Materials Technology Series, I.B. Cadoff and E. Miller, ed.; Reinhold Publishing Cooperation, New York, 1960; pp. 199–226).
82. L.I. Anatychuk, O.J. Luste, and L.N. Vikhor: Optimal functions as an effective method for thermoelectric devices design. In *Fifteenth International Conference on Thermoelectrics*, edited by J.-P. Fleurial (IEEE, 1996; pp. 223–226).
83. L.I. Anatychuk and L.N. Vikhor: Functionally graded materials and new prospects for thermoelectricity use. In *Proceedings ICT '97. Sixteenth International Conference on Thermoelectrics*, edited by Armin Heinrich Joachim Schumann (IEEE, 1997; pp. 588–591).
84. T.P. Hogan and T. Shih: Modeling and characterization of power generation modules based on bulk materials. In *CRC Handbook of Thermoelectrics: Macro to Nano* (D.M. Rowe, ed.; Taylor & Francis, Boca Raton, FL, 2006; chap. 12).
85. M.H. Norwood: A comparison of theory and experiment for a thermoelectric cooler. *J. Appl. Phys.* **32**, 2559–2563 (1961).
86. M. Power and R.A. Handelsman: Generalized calculation of thermoelectric efficiency. *Adv. Energy Convers.* **1**, 45–60 (1961).
87. M. Chen, L.A. Rosendahl, T.J. Condra, and J.K. Pedersen: Numerical modeling of thermoelectric generators with varying material properties in a circuit simulator. *IEEE Trans. Energy Convers.* **24**, 112–124 (2009).
88. D.M. Rowe and G. Min: Evaluation of thermoelectric modules for power generation. *J. Power Sources* **73**, 193–198 (1998).
89. A. Jacquot, M. Jägle, J. König, D.G. Ebling, and H. Böttner: Theoretical study of the Harman method for evaluating the thermoelectric performance of materials and components at high temperature. In *Proceedings of the 5th European Conference on Thermoelectrics* (2007).
90. M. Jägle: Simulating thermoelectric effects with finite element analysis using COMSOL. In *Proceedings of the 5th European Conference on Thermoelectrics* (2007).
91. A. López, F. Villasevil, G. Noriega, and D. Platzek: Thermoelectric integrated numerical modeling process of a temperature and humidity control device apply to vehicles for fogging preventing. In *Proceedings of the 5th European Conference on Thermoelectrics* (2007).
92. M. Freunek, M. Müller, T. Ungan, W. Walker, and L.M. Reindl: New physical model for thermoelectric generators. *J. Electro. Mater.* **38**, 1214–1220 (2009).
93. G. Fraisse, M. Lazard, C. Goupil, and J.Y. Serrat: Study of a thermoelement's behaviour through a modelling based on electrical analogy. *Int. J. Heat and Mass Transfer* **53**, 3503–3512 (2010).
94. A.M. Morega, M. Morega, and M.A. Panait: Structural optimization of a thermoelectric generator by numerical simulation. *Rev. Roum. Sci. Tech. Serie Électrotech. Énergétique* **55**, 3–12 (2010).
95. E. Sandoz-Rosado and R. Stevens: Robust finite element model for the design of thermoelectric modules. *J. Electron. Mater.* **39**, 1848–1855 (2010).
96. D. Ebling, K. Bartholomé, M. Bartel, and M. Jägle: Module geometry and contact resistance of thermoelectric generators

https://doi.org/10.1557/jmr.2011.91 Published online by Cambridge University Press

analyzed by multiphysics simulation. *J. Electron. Mater.* **39**, 1376–1380 (2010).
97. E.W. Weisstein: Bessel function. From *MathWorld*–A Wolfram Web Resource. http://mathworld.wolfram.com/Bessetfunction.html/
98. E.W. Weisstein: Sine integral. From *MathWorld*–A Wolfram Web Resource. http://mathworld.wolfram.com/SineIntegral.html
99. E.W. Weisstein: Cosine integral. From *MathWorld*–A Wolfram Web Resource. http://mathworld.wolfram.com/CosineIntegral.html
100. E.W. Weisstein: Dilogarithm. From *MathWorld*–A Wolfram Web Resource. http://mathworld.wolfram.com/Dialogarithm.html.
101. G.N. Watson: *A Treatise on the Theory of Bessel Functions* (Cambridge University Press, London, 1922).

APPENDIX A: TRANSFORMATION OF THE THERMAL ENERGY BALANCE AND ITS SOLUTION EXPRESSED IN SPECIAL FUNCTIONS

The thermal energy balance Eg. (2b) can be written in another notation where it shows

$$[a(\kappa)\xi_\kappa + b(\kappa)x]T'(x) + b(\kappa)T'(x) - jb(S)T(x) = -j^2[a(\sigma)\xi_\sigma + b(\sigma)x]^{-1} \quad , \quad \text{(A1)}$$

with the abbreviations

$$a(y) = \frac{2y_{\text{av}}}{1+\xi_y} \quad \text{and}$$

$$b(y) = \frac{2y_{\text{av}}}{L}\frac{(1-\xi_y)}{(1+\xi_y)} = \frac{\Delta y}{L}$$

$$\text{with} \quad y = \kappa, \sigma, S \quad .$$

As one easily sees the b gives the appropriate slope, e.g., $\kappa'(x) = b(\kappa)$. There is another form of writing the material profiles with the chosen abbreviations, e.g., $\kappa = a(\kappa)\xi_\kappa + b(\kappa)x$. To derive the Bessel equation from the (homogeneous part of the) thermal energy balance [see Eq. (A1)], we used the following substitution:

$$z = -2\sqrt{\frac{-jb(S)}{b^2(\kappa)}}\sqrt{\kappa(x)} \equiv A\sqrt{\kappa(x)} \quad , \quad \text{(A2)}$$

leading to $T''(z) + z^{-1}T'(z) + T(z) = 0$ for the homogeneous part of Eq. (A1), which is equivalent to a Bessel equation of order 0 (after multiplying with z^2).

The complete inhomogeneous differential equation can be calculated to

$$T''(z) + z^{-1}T'(z) + T(z) = \frac{j}{b(S)\sigma_{\text{av}}} \quad . \quad \text{(A3)}$$

A1. Bessel functions

Some properties of Bessel functions are helpful in calculating the performance parameters,[97] f.i. $J'_0(z) = -J_1(z)$, which leads in our case to

$$\frac{d}{dx}\left[J_0\left(A\sqrt{\kappa(x)}\right)\right] = -\frac{Ab(\kappa)}{2\sqrt{\kappa(x)}}J_1\left(A\sqrt{\kappa(x)}\right) \quad . \quad \text{(A4)}$$

The integral of the Bessel function gives

$$\int J_0\left(A\sqrt{\kappa(x)}\right)dx = \frac{2\sqrt{\kappa(x)}}{Ab(\kappa)}J_1\left(A\sqrt{\kappa(x)}\right) \quad . \quad \text{(A5)}$$

Analogous relations are found for the Bessel function of the second kind $Y_0(z)$.

A2. Sine and cosine integral

Here, $\text{Si}(x)$ and $\text{Ci}(x)$ are the respective sine and cosine integral[98,99]

$$\text{Si}(x) = \int_0^x \frac{\sin(y)}{y}dy \quad \text{and} \quad \text{Ci}(x) = \gamma + \ln(x) + \int_0^x \frac{\cos(y)-1}{y}dy \quad , \quad \text{(A6)}$$

with Euler's constant γ.

A3. Dilogarithm function

The function $\text{Li}_2(z)$ is the dilogarithm function[100] defined as

$$\text{Li}_2(z) = \sum_{k=1}^{\infty}\frac{z^k}{k^2} \quad \text{or} \quad \text{Li}_2(z) \equiv \int_z^0 \frac{\ln(1-t)}{t}dt \quad . \quad \text{(A7)}$$

A more detailed discussion and a number of relations can be found in Refs. 56–60 and 97–101 and references therein.

https://doi.org/10.1557/jmr.2011.91 Published online by Cambridge University Press